A Closed-Loop Simulation on Regional Modelling of Gravity Changes from GRACE

Katrin Bentel and Christian Gerlach

Abstract

A closed-loop simulation is set up in order to study in detail regional gravity modelling from GRACE-type observations. Thereby, potential differences between two satellites are simulated from a pre-defined mass trend signal, superimposed to a static background gravity model. These simulated observations are used for regional gravity field analysis with spherical radial basis functions. Finally, we use EOF analysis to identify the trend in gravity potential from a time series of 15-days quasi-static snapshots. Regional gravity modelling on the sphere is fairly complex and introduces approximation errors and artificial effects. In order not to mix up these errors with noise from the observations, we currently use noise-free observations. The model provides a versatile tool for detailed investigation of the data analysis method. Validation of the results is performed by comparison of input and output gravity change.

Keywords

Regional gravity modelling • Radial basis functions • EOF analysis • Closed-loop simulation

1 Introduction

Observations of mass changes in the Earth system play an important role in many disciplines. Especially, mass changes in the cryosphere gain more and more interest because the cryosphere is considered to be very sensitive to a changing climate.

Good temporal and spatial coverage with terrestrial observations of mass changes is almost impossible. Alternatively, airborne remote sensing provides high spatial resolution, but continuous monitoring is still not possible. Satellite techniques offer continuous observations while the satellite is in orbit and the instruments in operation. Coverage, temporal as well as spatial, depends on the orbit of the satellite. A wide range of different methods is used for investigation of mass changes from space.

We want to focus on mass changes from gravity observations of the GRACE (Gravity Recovery And Climate Experiment) satellite mission (see Tapley et al. 2004). The GRACE mission was launched in 2002 and is still operational today. Thus, it provides very long and valuable time series of observations. However, the main drawback is signal damping at the satellites' orbit height which limits the spatial resolution. Global solutions from the GRACE mission are provided in spherical harmonic basis functions and are successfully used to monitor ice mass changes in Greenland and Antarctica, the Earth's largest ice-covered areas. See for example Ramillien et al. (2006) and Velicogna (2009) amongst many others. In contrast to the global approach, spherical radial basis functions with local support may be used for better regional gravity field representations. Klees et al. (2008) give an overview of different types of possible functions.

K. Bentel (✉)
Department of Mathematical Sciences and Technology, Norwegian University of Life Sciences, IMT, Postboks 5003, 1432 Ås, Norway
e-mail: katrin.bentel@umb.no

C. Gerlach
Bavarian Academy of Sciences, Kommission für Erdmessung und Glaziologie, Munich, Germany

C. Rizos and P. Willis (eds.), *Earth on the Edge: Science for a Sustainable Planet*, International Association of Geodesy Symposia 139, DOI 10.1007/978-3-642-37222-3_11,

The fundamentals of modelling in radial basis functions can be found in Freeden et al. (1998) or Holschneider et al. (2003). Finally, different approaches for gravity modelling in spherical radial basis functions are given, for example, in Schmidt et al. (2007) or Freeden and Schreiner (2005).

In the interpretation of the results it has to be considered that satellite gravity measurements monitor all mass changes in the Earth system. Mass changes from the cryosphere, the atmosphere, the ocean, continental hydrology, or glacial isostatic processes are superimposed and need to be separated from each other. Assuming individual spatial and temporal characteristics of the different mass change components, we propose EOF (Empirical Orthogonal Function) analysis. Fundamentals of this method are found in Preisendorfer (1988) or Jolliffe (2002) and applications for GRACE gravity data for example in Schrama et al. (2007) and Rangelova et al. (2007).

2 Global Versus Regional Gravity Modelling

The GRACE mission consists of two satellites at about 450 km orbit height which are about 220 km apart from each other. The core measurements of GRACE are precise range-rates between the two satellites, measured with a K-band microwave instrument. These are available as Level-1B data products, along with GPS measurements of the satellites' positions, information from attitude sensors, and accelerometer measurements. Derived science products are monthly global gravity maps (Level-2 data), see Tapley et al. (2004) and Flechtner et al. (2007). These monthly solutions are represented in spherical harmonics and are best fitting the data on a global scale. Thus, they are not necessarily optimal solutions for a specific region. This also means that small regional gravity signals, which might actually be detected by the K-band range-rates, could be masked in the global solutions.

Therefore, we study regional gravity field analysis from GRACE observations (derived from Level-1B data) which allow for an optimal solution in a particular region. For the parametrization we use spherical radial basis functions which have quasi-local support and are rotationally symmetric. This means, their amplitude decreases rapidly with distance from their center and, thus, the basis functions' influence is maximal at the location of the center and has very little influence in non-local areas.

3 Closed Loop Model

Regional representation of the Earth's gravity field from GRACE Level-1B data is not straightforward. Additionally, determination of mass changes from satellite gravimetry is a challenge due to the downward continuation problem and the question of separation of sources. In order to investigate data analysis methods in more detail, and to have control over error effects due to the methods in use, we set up a closed-loop simulation which is illustrated in Fig. 1.

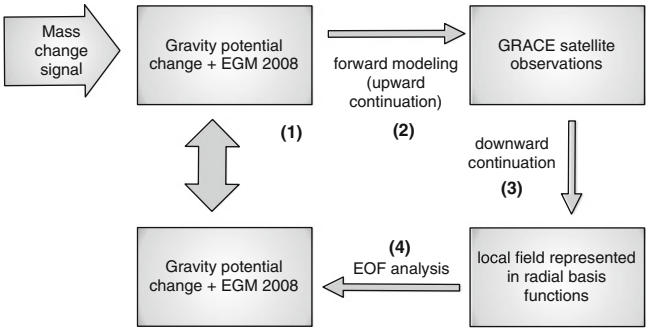

Fig. 1 Illustration of the closed-loop model

The first step of the closed-loop simulation is the choice of a time-variable input gravity signal. In the second step, potential differences between the GRACE satellites are synthesized from this signal. These are taken as observations in the simulation. Spherical radial basis functions are used for the analysis and regional modelling in step three. This step also contains the downward continuation and the result is a regional gravity solution on the sphere for every 15 days. Since this signal contains all different mass change effects from Earth, or, in this simulation, the predefined gravity change and a background signal from a global geopotential model (EGM2008), a signal separation step is needed. Thus, EOF analysis is step four in the simulation where we try to recover the input gravity trend. Finally, comparison of the input and the recovered signal is an easy tool to evaluate the performance of the analysis steps. In the following subsections steps one to four are explained in more detail.

3.1 Cryosphere Signal Modelled by a Mascon

GRACE observations have been very successfully used by Luthcke et al. (2008) to determine glacier mass changes in the Alaska Range region. They use a mascon (mass concentration) parametrization of the gravity field variations. Thereby, a small uniform layer of mass over a region at an epoch t can be represented in a set of differential Stokes coefficients as described in Eq. (1). These sets of differential coefficients provide an improvement in the representation in spherical harmonics for the area of interest for a given time interval and can be computed from mascon area and height according to:

$$\begin{Bmatrix} \Delta C_{lm}(t) \\ \Delta S_{lm}(t) \end{Bmatrix} = \frac{(1+k_l)R^2\sigma(t)}{(2l+1)M_e} \int \bar{P}_{lm}(\sin\vartheta) \begin{Bmatrix} \cos \\ \sin \end{Bmatrix} m\lambda \; d\Omega \tag{1}$$

Hereby, k_l is the Love number of degree l, R is the radius of the Earth with $R = 6,378,137\,\text{m}$, M_e is the mass of the Earth with $M_e = 5.9736e24\,\text{kg}$, and $\bar{P}_{lm}$ are the normalized Legendre functions. The mascon area is given by the solid-angle surface area Ω, and its thickness via $\sigma(t)$, a parameter which is directly linked to the mascon height in meters and can change with time t. It holds $d\Omega = \cos(\vartheta)\, d\vartheta\, d\lambda$ and the integration is performed only over the area of the mascon. We use equivalent water height to convert a certain mass into the height information for the mascon area.

As a signal example, we choose an annual regional mass loss of 3 Gt, a value which is roughly in the order of magnitude of the signal from Austfonna, Svalbards largest ice cap (see Dowdeswell et al. 2008). This mass loss leads to a 15-day height decrease of 0.0031 m in a 2° by 2° mascon at a latitude of 35°, respectively, a decrease in gravity potential on the sphere of approximately $3.4522 \cdot 10^{-5}\,\text{m}^2/\text{s}^2$ per year, as directly found from spherical harmonic synthesis from the mascon coefficients and degrees 10–120. This degree range corresponds to the forward modelled signal, see Sect. 3.2.

3.2 Forward Modelling

The second step is the simulation of GRACE-type potential differences at orbit height for the previously defined mass-loss signal in addition to a background signal, the global geopotential model EGM 2008. Mascon and background signal are used in a spherical harmonic synthesis from degree 10 to 120. A synthesis of the signal only from degree 10 simulates removing the long wavelengths part of the signal. We locate the mascon (Sect. 3.1) in the Himalayan area, from 84° to 86° longitude and 34° to 36° latitude. This location is a challenging location for our closed-loop model in terms of detecting the mascon signal since the gravity signal from topography is very high in the Himalayas and the quality of a regional gravity representation on the sphere depends on the signal magnitude in the area because of boundary and oscillation effects. From the mascon and geopotential model we compute the resulting gravity potential at both satellites GRACE A and GRACE B for every 5 s. In this simulation, we simulate one GRACE-type orbit and use this orbit for both satellites, GRACE A and B, following each other at a distance of about 220 km or about 30 s. From GRACE Level-1B data, gravity potential differences between the two spacecraft can be obtained via the so-called energy integral approach (e.g. Visser et al. 2003). The potential differences are taken as observations in our model. We use noise-free simulated observations in order to study details of the modelling process and to avoid effects from the regional modelling process itself being covered by noise from the observations. The approximation in Eq. (2) relates instantaneously the GRACE inter-satellite range-rate measurements $\dot{\rho}_{12}$ to gravitational potential differences along the orbit between GRACE A and B.

$$V_2 - V_1 \equiv V_{12} \approx |\dot{\mathbf{x}}_1|\dot{\rho}_{12} \tag{2}$$

V_1 and V_2 are gravity potential at the two satellites, and V_{12} is the potential difference between them. $\dot{\mathbf{x}}_1$ is the velocity vector of one of the two satellites. This approximate model is used and explained in Han (2003, Eq. (4)), and Jekeli (1999, Eq. (25)), and references herein. It was initially developed by Wolff (1969).

3.3 Representation in Radial Basis Functions

The next step in the closed-loop model is the analysis of the simulated observations. While we use mascon parametrization in the forward model, we propose spherical radial basis function to analyze the simulated observations. For a regional representation in spherical radial basis functions, multiple copies of a radial basis function are located at grid points covering the area of interest. We use Shannon scaling functions and Fig. 2 shows a radial basis function ($B(\mathbf{x}, \mathbf{x}_k)$) together with a Reuter grid (see e.g. Schmidt et al. 2007; Freeden et al. 1998) for our area of interest. Equation (3) gives a general representation of a signal F in radial basis functions. Hereby $\mathbf{x}_k$ are the grid points, and N is the number of grid points under consideration. $\mathbf{x} = r\,[\cos\phi\,\cos\lambda,\ \cos\phi\,\sin\lambda,\ \sin\phi]'$. In Eq. (4), the formula for a radial basis function $B(\mathbf{x}, \mathbf{x}_k)$ is given, and in Eq. (6) the observational equation which we use.

$$F(\mathbf{x}) = \sum_{k=1}^{N} d_k\, B(\mathbf{x}, \mathbf{x}_k) \tag{3}$$

$$B(\mathbf{x}, \mathbf{x}_k) = \sum_{n=0}^{n''} \frac{2n+1}{4\pi R^2} \left(\frac{R}{r}\right)^{n+1} B_n\, P_n(\cos(\vartheta)). \tag{4}$$

r is the geocentric distance of the observation point and R is the radius of the sphere with $R = 6,378,137\,\text{m}$. The term $(R/r)^{n+1}$ allows for downward continuation of the observed signal from satellite altitude (r) to the sphere (R). P_n are the Legendre polynomials where ϑ is the spherical distance between $\mathbf{x}$ and $\mathbf{x}_k$, and B_n are coefficients which specify the radial basis function. The coefficients B_n also give the frequency behaviour of the radial basis function, and for the Shannon scaling function it holds

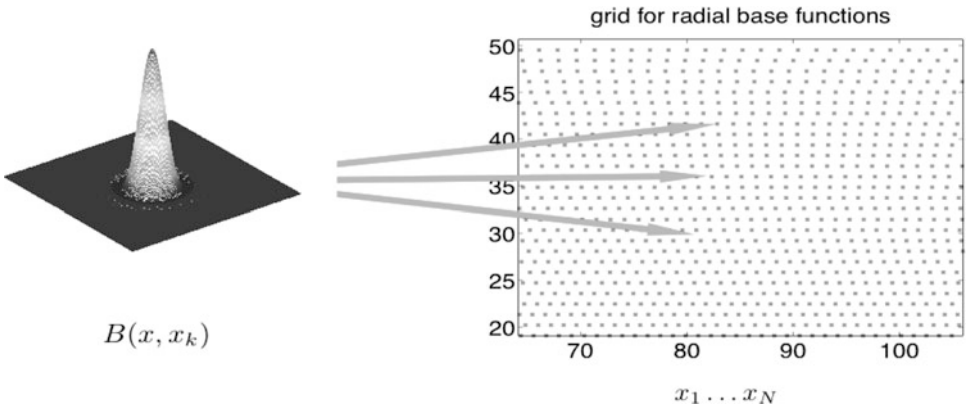

Fig. 2 Location of radial basis functions on a Reuter grid

$$B_n = \begin{cases} 1 & \forall \quad n \leq n_{\max} \\ 0 & \forall \quad n > n_{\max}. \end{cases} \tag{5}$$

We use $n_{\max} = 130$ and a spacing between the individual grid points in the Reuter grid of about 1.125°. The maximum degree in the kernel has to be at least as high as the maximum degree in the signal to be represented, and previous experiments have shown that a slightly higher maximum degree in the kernel than in the signal leads to a better representation of the signal. The spacing in the Reuter grid is derived form the maximum degree in the kernel.

The potential difference V_{12} (Eq. (2)) can be written as:

$$V_{12} = \sum_{k=1}^{N} d_k (B(\mathbf{x}_2, \mathbf{x}_k) - B(\mathbf{x}_1, \mathbf{x}_k)) \tag{6}$$

Hereby $\mathbf{x}_1$ is the position of satellite A and $\mathbf{x}_2$ the position of satellite B.

The estimation of the coefficients d_k is an inverse problem and the observational matrix is singular because of two reasons: first, more radial basis functions are used in the representation than minimally needed. With the minimum number of basis functions, which is derived from a global point of view, no satisfying representation of the regional signal can be achieved. The point grid also imposes constraints on the number of basis functions due to its structure. Second, the system of observation equations for the signal F is singular due to the downward continuation problem which is included. The singular system is solved by using a pseudoinverse of the normal equation matrix. The pseudoinverse is based on a singular value decomposition.

After estimation of the coefficients d_k, they can be used in a synthesis step to reconstruct the regional gravity field on the sphere. This is performed for every 15 days, since we have found that in the course of 15 days we have enough observations in the area of interest to estimate the coefficients d_k. Finally, after the downward continuation, we have a time series of gridded potential values on the sphere.

3.4 Identification of the Cryosphere Signal

The last step, after a regional gravity signal on the sphere has been determined for every 15 days (which is possible at an accuracy of 3.73 %, percentage of the residuals root mean square from the signal root mean square), is separation of sources. In this basic simulation, the gravity change trend needs to be identified. We propose Empirical Orthogonal Function (EOF) analysis, which has been successfully used to separate different gravity signals by, for example, Schrama et al. (2007) and Rangelova et al. (2007). Even though we just want to identify a trend, we still use this method, since we are planning to use our closed-loop model with more realistic simulated observations later on. In the EOF analysis, different types of signals are identified according to their spatial and temporal correlations. White noise is assumed to have no correlations at all. The method is based on a singular value decomposition. It gives a set of modes, and each of them consists of three elements: purely spatial information (left eigenvectors), purely temporal information (right eigenvectors), and information about the magnitude, which is given by the singular value. The left and right eigenvectors, also called EOF patterns and principal components, are normalized vectors, and the only scaling information is contained in the singular values. Multiplication of the three elements gives the signal which is represented by the mode. The most dominant signal will have the largest singular value and is therefore mapped into mode one. The following modes contain other signals, which could be identified, in the order of their signal strength.

Figure 3 shows the first three modes from the EOF analysis of our recovered signal. On the left, there are the spatial patterns and on the right the temporal behaviour, both normalized. The static background signal does not appear anymore, since the mean has been removed and only signal variations are decomposed in the EOF analysis.

The spatial structure in the first mode shows the pattern which we expect from the mass loss signal modelled by the mascon. The signal clearly originates from the square in the center of the region. The temporal behaviour corresponds

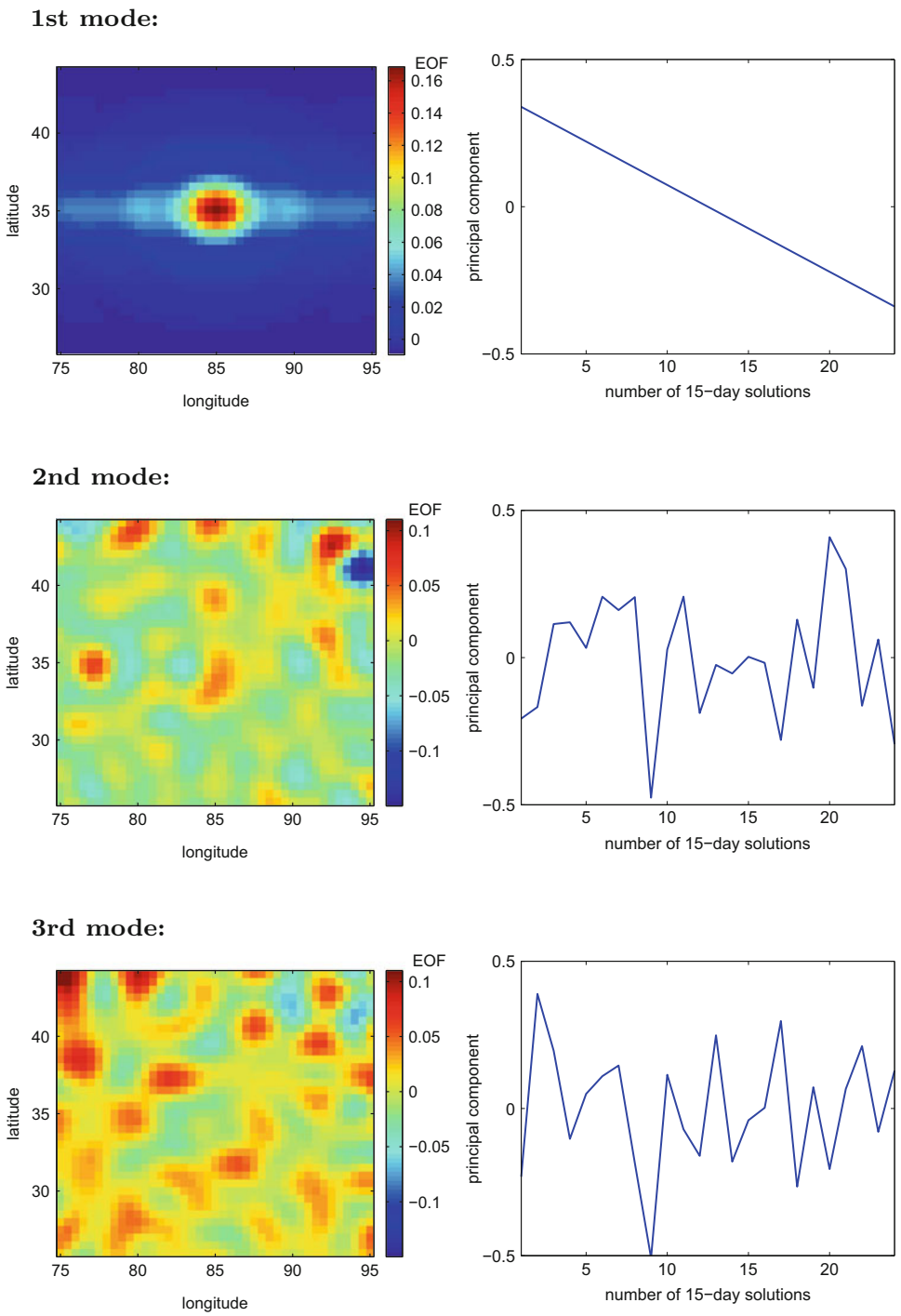

Fig. 3 First three modes from the EOF analysis. 1st mode: singular value $2.93 \cdot 10^{-4}$ (m^2/s^2). 2nd mode: singular value $1.83 \cdot 10^{-7}$ (m^2/s^2). 3rd mode: singular value $1.79 \cdot 10^{-7}$ (m^2/s^2)

as well to what we have modelled, the curve indicates a continuous mass loss. The detection of the trend is that perfect because we did not consider noise and other signals in our modelling.

The most interesting issue, however, is if we can reconstruct our input mass loss. To reconstruct the signal from mode 1, we multiply the three components of the mode. From the spatial pattern we chose the maximum value in the center of the peak. From the trend, we take the maximum and minimum values. The decrease in gravity potential indicated by the trend from $0.1686 \cdot 2.9250 \cdot 10^{-4} \cdot 0.3391\,m^2/s^2$ to $0.1686 \cdot 2.9250 \cdot 10^{-4} \cdot (-0.3390)\,m^2/s^2$ is about $\mathbf{-3.3441 \cdot 10^{-5}}\,m^2/s^2$. Referring back to Sect. 3.1, this corresponds to the decrease in gravity potential ($\mathbf{-3.4522 \cdot 10^{-5}}\,m^2/s^2$) which was modelled by the mascon as input signal and can be recovered with an error of 3.12 %.

A trend recovery with an error level of a few percent is a fairly good result compared to other studies on ice

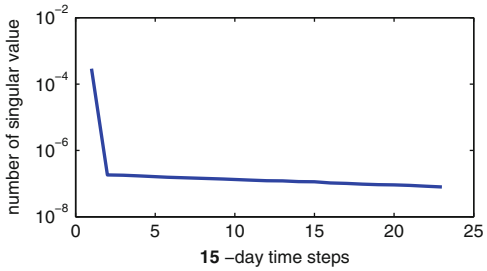

Fig. 4 Singular values from the EOF analysis

mass changes from GRACE observations, see, for example, Schrama and Wouters (2011) and references therein, where ice mass changes can only be detected with uncertainties of roughly about 10 %. Of course, one has to keep in mind that we used noise-free observations in our simulation.

In the following two modes no signal structure can be recognized. The spatial patterns as well as the temporal behaviour seem to be purely random. This corresponds to what we would expect, since there was no other signal used in the simulation than the constant background signal and the mass trend. The idea that these two modes, as well as all higher modes, are only noise is also confirmed by the singular values. The singular values of modes two and three are of the same order of magnitude and significantly, that is about three orders of magnitude, lower than the singular value of the first mode. All modes that contain only white noise are expected to have about the same singular value, and it is expected that this value is fairly low compared to the signal containing modes. Figure 4 gives a plot of all singular values. This plot shows that all modes, but the first one, have about the same singular values, and thus, we conclude that these modes are all noise containing modes.

4 Summary and Outlook

The closed-loop simulation provides a very helpful tool to investigate the method of regional gravity modelling with spherical radial basis functions from GRACE Level-1 data. In the regional modelling procedure a lot of parameters have to be chosen. These are the radial basis function, the point grid, and the method for the solution of the inverse problem. Also, the downward continuation problem needs to be treated appropriately. The errors in the reconstructed gravity field due to the downward continuation problem are much larger than the differences in the results from the choice of different radial basis functions. Even though the Shannon kernel is probably the most simple radial basis function, it is therefore still appropriate to use in our simulations.

With the model, we can study in detail all strengths and shortcomings of our analysis method, and hopefully develop a valuable tool for analyzing real data at a later stage. We will be able to distinguish between effects which actually originate from the data, and such ones, which are artificial effects due to the methods in use. In our future work, we want to introduce a realistic level of noise in the model. In a previous study, Bentel and Gerlach (2010), we have shown that a certain level of white noise on the range rates generates geoid error degree variances which are very similar to those from a simple coloured noise mode, which represents real GRACE error degree variances. Therefore, the next step will be to use a realistic level of white noise on the observations. Unfortunately, only an unrealistically low level of white noise on the observations was possible in order to still recover the mass trend signal. We plan to implement an appropriate filtering step, so that we can use a realistic signal-to-noise ratio. Even though regional modelling with the Shannon scaling function provides filtering in the frequency domain and EOF analysis implies separation of signal from white noise, this does not seem to be sufficient for a realistic noise level.

When approaching the analysis of real data later on, a very important issue is the appropriate separation of sources, mainly to separate actual ice mass loss from post glacial rebound effects and others. It might be advisable to use a closed-loop model for a comprehensive study of separability of sources as well.

References

Bentel K, Gerlach C (2010) Observability of regional cryosphere signals with satellite gravity missions of GRACE-type. In: Lacoste-Francis H (ed) Proceedings of the ESA living planet symposium special publication SP-686. ESA Communications, ESTEC, The Netherlands

Dowdeswell JA, Benham TJ, Strozzi T, Hagen JO (2008) Iceberg calving flux and mass balance of the Austfonna ice cap on Nordaustlandet, Svalbard. J Geophys Res 113. doi:10.1029/2007JF000905

Flechtner F, Bettadpur S, Watkins M, Kruizinga G (2007) GRACE science data system monthly report January 2007. Tech. rep., GFZ Potsdam

Freeden W, Schreiner M (2005) Spaceborne gravitational field determination by means of locally supported wavelets. J Geodes 79:431–446

Freeden W, Gervens T, Schreiner M (1998) Constructive approximation on the sphere with applications to geoscience. Oxford Science Publications, Oxford

Han SC (2003) Efficient determination of global gravity field from satellite-to-satellite tracking mission. Celest Mech Dynam Astron 88:69–102

Holschneider M, Chambodut A, Mandea M (2003) From global to regional analysis of the magnetic field on the sphere using wavelet frames. Phys Earth Planet Inter 135(2–3). doi:10.1016/S0031-9201(02)00210-8

Jekeli C (1999) The determination of gravitational potential differences from satellite-to-satellite tracking. Celest Mech Dynam Astron 75:85–101

Jolliffe IT (2002) Principal component analysis. Springer series in statistics, 2nd edn. Springer, New York

Klees R, Tenzer R, Prutkin I, Wittwer T (2008) A data-driven approach to local gravity field modelling using spherical radial basis functions. J Geodes 82(8). doi:10.1007/s00190-007-0196-3

Luthcke SB, Arendt AA, Rowlands DD, McCarthy JJ, Larsen CF (2008) Recent glacier mass changes in the Gulf of Alaska region from GRACE mascon solutions. J Glaciol 54:1–11

Preisendorfer RW (1988) Principal component analysis in meteorology and oceanography. Developments in atmospheric sciences, vol 17. Elsevier, Amsterdam

Ramillien G, Lombard A, Cazenave A, Ivins E, Llubes M, Remy F, Biancale R (2006) Interannual variations of the mass balance of the Antarctica and Greenland ice sheets from GRACE. Global Planet Change 53(3):198–208

Rangelova E, van der Wal W, Braun A, Sideris MG, Wu P (2007) Analysis of gravity recovery and climate experiment time-variable mass redistribution signals over North America by means of principal component analysis. J Geophys Res 112. doi:10.1029/2006JF000615

Schmidt M, Fengler M, Mayer-Gürr T, Eicker A, Kusche J, Sánchez L, Han SC (2007) Regional gravity modeling in terms of spherical base functions. J Geod. doi:10.1007/s00190-006-0101-5

Schrama EJO, Wouters B (2011) Revisiting Greenland ice sheet mass loss observed by GRACE. J Geophys Res 116. doi:10.1029/2009JB006847

Schrama EJO, Wouters B, Lavalleé DA (2007) Signal and noise in gravity recovery and climate experiment (GRACE) observed surface mass variations. J Geophys Res 12. doi:10.1029/2006JB004882

Tapley B, Bettadpur S, Watkins M, Reigber C (2004) The gravity recovery and climate experiment: mission overview and early results. Geophys Res Lett 31(L09607). doi:10.1029/2004GL019920

Velicogna I (2009) Increasing rates of ice mass loss from the Greenland and Antarctic ice sheets revealed by GRACE. Geophys Res Lett 36(19). doi:10.1029/2009GL040222

Visser P, Sneeuw N, Gerlach C (2003) Energy integral method for gravity field determination from satellite orbit coordinates. J Geodes 77:207–216

Wolff M (1969) Direct measurements of the Earth's gravitational potential using a satellite pair. J Geophys Res 74(22):5295–5300